IEEE Access
Multidisciplinary | Rapid Review | Open Access Journal

Received February 14, 2020, accepted March 3, 2020, date of publication March 6, 2020, date of current version March 17, 2020.

Digital Object Identifier 10.1109/ACCESS.2020.2979141

Novel Nonlinear Hypothesis for the Delta Parallel Robot Modeling

GUSTAVO AQUINO, JOSÉ DE JESÚS RUBIO, (Member, IEEE), JAIME PACHECO, GUADALUPE JULIANA GUTIERREZ, GENARO OCHOA, RICARDO BALCAZAR, DAVID RICARDO CRUZ, ENRIQUE GARCIA, JUAN FRANCISCO NOVOA, AND ALEJANDRO ZACARIAS

Sección de Estudios de Posgrado e Investigación, ESIME Azcapotzalco, Instituto Politécnico Nacional, Mexico City 02250, Mexico

Corresponding author: José de Jesús Rubio (rubio.josedejesus@gmail.com)

ABSTRACT In previous investigations, the nonlinear hypothesis use the linear bounded maps. Nonlinear hypothesis are described as the combination of the first order terms, and after of the mentioned combination, one bounded map is applied to alter the result. This document proposes two nonlinear hypothesis which use different structures instead of using the linear bounded maps. They are termed as novel nonlinear hypothesis and second order nonlinear hypothesis and their goal is to improve the second order processes modeling. The proposed nonlinear hypothesis are described as the combination of the first order and second order terms. Since the delta parallel robot is a second order process, it is an excellent platform to prove the effectiveness of the two proposed hypothesis.

INDEX TERMS Novel nonlinear hypothesis, second order nonlinear hypothesis, nonlinear hypothesis, delta parallel robot.

I. INTRODUCTION

In the last few years, artificial intelligence has permeated many aspects of the lives such as the modeling [1]–[3] and optimization [4]–[6]. There are two important approaches of the artificial intelligence used for the modeling like the fuzzy models and neural networks. The fuzzy models and neural networks require of hypothesis containing the membership and activation maps for their acceptable performance. Since all the membership and activation maps are bounded, they are called bounded maps. This document is focused in hypothesis containing bounded maps for the modeling.

There exist several interesting investigations about hypothesis containing bounded maps for the modeling. In [7], [8], authors use hypothesis containing linear membership maps. In [9], [10], authors use hypothesis containing triangular membership maps. In [11], [12], authors use hypothesis containing trapezoidal membership maps. In [13], [14], authors use hypothesis containing Gaussian membership maps. In [15], [16], authors use hypothesis containing linear activation maps. In [17], [18], authors use hypothesis containing discontinuous activation maps. In [19], [20], authors use hypothesis containing sigmoid activation maps. In [21], [22], authors use hypothesis containing hyperbolic tangent activation maps. In [23], [24], authors use hypothesis containing relu activation maps. In [25], [26], authors use hypothesis containing sign-bi-power activation maps.

From the above mentioned investigations, all nonlinear hypothesis part from the linear bounded maps like the linear membership maps of [7], [8], or the linear activation maps of [15], [16]. Nonlinear hypothesis are described as the combination of the first order terms and it is detailed as the sum of the multiplication of the first order modeling parameters with the first order inputs, and after of the mentioned combination, one bounded map like the sigmoid [19], [20], hyperbolic tangent [21], [22], Gaussian [13], [14], or other is applied to alter the result.

It is important to notice that in previous investigations, the nonlinear hypothesis use the linear bounded maps. This document proposes two nonlinear hypothesis which use different structures instead of using the linear bounded maps. They are termed as novel nonlinear hypothesis and second order nonlinear hypothesis and their goal is to improve the second order processes modeling. The proposed nonlinear hypothesis are described as the combination of the first order and second order terms and it is detailed as the sum of the

The associate editor coordinating the review of this manuscript and approving it for publication was Wei-Chang Yeh.

multiplications of the first order modeling parameters with the first and second order inputs. The steps of this design are as follows:

1) One of the next four hypothesis is chosen for the second order processes modeling: 1) a linear hypothesis, it considers the sum of multiplication of the first order modeling parameters with the first order inputs, 2) a nonlinear hypothesis of previous investigations, it considers the sum of multiplication of the first order modeling parameters with the first order inputs, and after, one bounded map is applied to alter the result, 3) a second order nonlinear hypothesis, it considers the sum of multiplications of the first order modeling parameters with the first and second order inputs, and 4) a novel nonlinear hypothesis, it considers the sum of multiplications of the first order modeling parameters with the first and second order inputs, and multiplications of the first order modeling parameters with the cross first and second order inputs. In all the hypothesis, the gradient is utilized for the updating.
2) Finally, since the delta parallel robot is a second order process, the nonlinear hypothesis of previous investigations, second order nonlinear hypothesis, and novel nonlinear hypothesis are applied for the modeling of the experimental linear and curve paths in a delta parallel robot. The delta parallel robot takes into account the behavior of the pick and place configuration. In this configuration, the delta parallel robot is utilized for the positioning of objects.

The document is structured in the next sentence. In Section II, the linear hypothesis, nonlinear hypothesis of previous investigations, second order nonlinear hypothesis, and novel nonlinear hypothesis are designed for the second order nonlinear processes modeling. In Section III, the experimental platform of the delta parallel robot is described. In Section IV, nonlinear hypothesis of previous investigations, second order nonlinear hypothesis, and novel nonlinear hypothesis are compared. Finally, in Section V conclusions and forthcoming works are explained.

II. HYPOTHESIS FOR THE SECOND ORDER PROCESSES MODELING

Since the delta parallel robot is a second order process, this section will design two variants of second order hypothesis denoted as novel nonlinear hypothesis and second order nonlinear hypothesis to improve the second order processes modeling, and the proposed nonlinear hypothesis will be compared with a nonlinear hypothesis of previous investigations. Since the delta parallel robot is a second order process, it will be used in a posterior section to prove the effectiveness of the two proposed hypothesis.

A. LINEAR HYPOTHESIS

A linear hypothesis is described as the combination of the first order terms and it is detailed as the sum of multiplication of the first order modeling parameters with the first order inputs [7], [8], [15], [16].

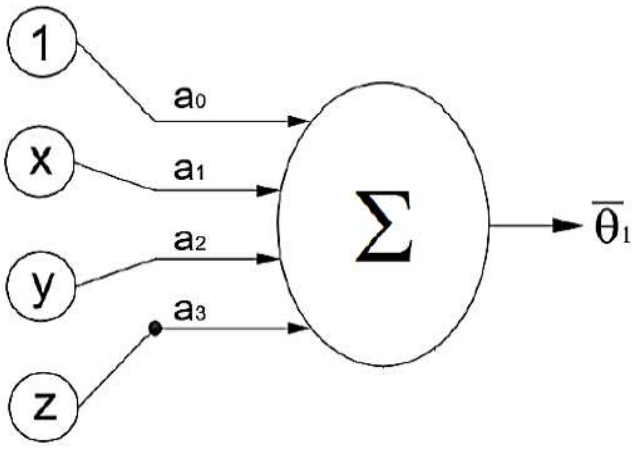

FIGURE 1. Structure of the linear hypothesis.

A linear hypothesis is described to relate the input variable of the end-effector $(x^i, y^i, z^i)^T$ with the output angles $(\theta_1^i, \theta_2^i, \theta_3^i)^T$ as:

$$\begin{aligned}\overline{\theta}_1^i &= a_0^i + a_1^i X_1^i + a_2^i X_2^i + a_3^i X_3^i \\ \overline{\theta}_2^i &= b_0^i + b_1^i X_1^i + b_2^i X_2^i + b_3^i X_3^i \\ \overline{\theta}_3^i &= c_0^i + c_1^i X_1^i + c_2^i X_2^i + c_3^i X_3^i \end{aligned} \tag{1}$$

where $i = 1, \ldots, m$, m is the data number, $X_0^i = 1$, $X_1^i = x$, $X_2^i = y$, $X_3^i = z$ are the inputs, $\overline{\theta}_1^i$, $\overline{\theta}_2^i$, $\overline{\theta}_3^i$ are estimated outputs, a_j^i, b_j^i, c_j^i, are modeling parameters to be updated, $j = 0, 1, 2, 3$. The goal is to find the modeling parameters a_j^i, b_j^i, c_j^i, such that $\overline{\theta}_1^i$, $\overline{\theta}_2^i$, $\overline{\theta}_3^i$ are near to θ_1^i, θ_2^i, θ_3^i.

Figure 1 shows the structure of the linear hypothesis for the output $\overline{\theta}_1^i$, it is similar for the outputs $\overline{\theta}_1^i$, $\overline{\theta}_3^i$.

The cost functions $J(a), J(b), J(c)$ are described as:

$$\begin{aligned} J(a) &= \frac{1}{2m}\sum_{i=1}^{m}\left(\overline{\theta}_1^i - \theta_1^i\right)^2 \\ J(b) &= \frac{1}{2m}\sum_{i=1}^{m}\left(\overline{\theta}_2^i - \theta_2^i\right)^2 \\ J(c) &= \frac{1}{2m}\sum_{i=1}^{m}\left(\overline{\theta}_3^i - \theta_3^i\right)^2 \end{aligned} \tag{2}$$

Utilizing the gradient, the updating for a_j^i, b_j^i, c_j^i are as:

$$\begin{aligned} a_j^{i+1} &= a_j^i - \alpha\frac{\partial J(a)}{\partial a_j} = a_j^i - \frac{\alpha}{m}\sum_{i=1}^{m}\left(\overline{\theta}_1^i - \theta_1^i\right)X_j^i \\ b_j^{i+1} &= b_j^i - \alpha\frac{\partial J(b)}{\partial b_j} = b_j^i - \frac{\alpha}{m}\sum_{i=1}^{m}\left(\overline{\theta}_2^i - \theta_2^i\right)X_j^i \\ c_j^{i+1} &= c_j^i - \alpha\frac{\partial J(c)}{\partial c_j} = c_j^i - \frac{\alpha}{m}\sum_{i=1}^{m}\left(\overline{\theta}_3^i - \theta_3^i\right)X_j^i \end{aligned} \tag{3}$$

where $i = 1, \ldots, m, j = 0, 1, 2, 3, \alpha$ is the modeling speed.

B. NONLINEAR HYPOTHESIS OF PREVIOUS INVESTIGATIONS

From the above mentioned investigations, all nonlinear hypothesis part from the linear bounded maps like the linear

membership maps of [7], [8], or the linear activation maps of [15], [16]. Nonlinear hypothesis are described as the combination of the first order terms and it is detailed as the sum of the multiplication of the first order modeling parameters with the first order inputs, and after of the mentioned combination, one bounded map like the sigmoid [19], [20], hyperbolic tangent [21], [22], Gaussian [13], [14], or other is applied to alter the result.

A nonlinear hypothesis of previous investigations is described to relate the input variable of the end-effector $(x^i, y^i, z^i)^T$ with the output angles $(\theta_1^i, \theta_2^i, \theta_3^i)^T$ as:

$$\begin{aligned}\overline{\theta}_1^i &= \varsigma_1^i\left(a_0^i + a_1^i X_1^i + a_2^i X_2^i + a_3^i X_3^i\right)\\ \overline{\theta}_2^i &= \varsigma_2^i\left(b_0^i + b_1^i X_1^i + b_2^i X_2^i + b_3^i X_3^i\right)\\ \overline{\theta}_3^i &= \varsigma_3^i\left(c_0^i + c_1^i X_1^i + c_2^i X_2^i + c_3^i X_3^i\right)\end{aligned} \tag{4}$$

where $i = 1, \ldots, m$, m is the data number, $X_0^i = 1$, $X_1^i = x$, $X_2^i = y$, $X_3^i = z$ are the inputs, $\overline{\theta}_1^i$, $\overline{\theta}_2^i$, $\overline{\theta}_3^i$ are estimated outputs, a_j^i, b_j^i, c_j^i, are modeling parameters to be updated, $j = 0, 1, 2, 3$. The goal is to find the modeling parameters a_j^i, b_j^i, c_j^i, such that $\overline{\theta}_1^i$, $\overline{\theta}_2^i$, $\overline{\theta}_3^i$ are near to θ_1^i, θ_2^i, θ_3^i. $\varsigma_1^i(\cdot)$, $\varsigma_2^i(\cdot)$, $\varsigma_3^i(\cdot)$ are bounded maps like the sigmoid, hyperbolic tangent, Gaussian, or other.

Figure 2 shows the structure of the linear hypothesis for the output $\overline{\theta}_1^i$, it is similar for the outputs $\overline{\theta}_1^i$, $\overline{\theta}_3^i$.

The cost functions $J(a)$, $J(b)$, $J(c)$ are described as:

$$\begin{aligned}J(a) &= \frac{1}{2m}\sum_{i=1}^{m}\left(\overline{\theta}_1^i - \theta_1^i\right)^2\\ J(b) &= \frac{1}{2m}\sum_{i=1}^{m}\left(\overline{\theta}_2^i - \theta_2^i\right)^2\\ J(c) &= \frac{1}{2m}\sum_{i=1}^{m}\left(\overline{\theta}_3^i - \theta_3^i\right)^2\end{aligned} \tag{5}$$

Utilizing the gradient, the updating for a_j^i, b_j^i, c_j^i are as:

$$\begin{aligned}a_j^{i+1} &= a_j^i - \alpha\frac{\partial J(a)}{\partial a_j}\\ &= a_j^i - \frac{\alpha}{m}\sum_{i=1}^{m}\left(\overline{\theta}_1^i - \theta_1^i\right)\varsigma_1^{i\prime}\left(a_0^i\right.\\ &\quad \left. + a_1^i X_1^i + a_2^i X_2^i + a_3^i X_3^i\right)X_j^i\\ b_j^{i+1} &= b_j^i - \alpha\frac{\partial J(b)}{\partial b_j}\\ &= b_j^i - \frac{\alpha}{m}\sum_{i=1}^{m}\left(\overline{\theta}_2^i - \theta_2^i\right)\varsigma_2^{i\prime}\left(a_0^i + a_1^i X_1^i\right.\\ &\quad \left. + a_2^i X_2^i + a_3^i X_3^i\right)X_j^i\\ c_j^{i+1} &= c_j^i - \alpha\frac{\partial J(c)}{\partial c_j}\\ &= c_j^i - \frac{\alpha}{m}\sum_{i=1}^{m}\left(\overline{\theta}_3^i - \theta_3^i\right)\varsigma_3^{i\prime}\left(a_0^i + a_1^i X_1^i\right.\\ &\quad \left. + a_2^i X_2^i + a_3^i X_3^i\right)X_j^i\end{aligned} \tag{6}$$

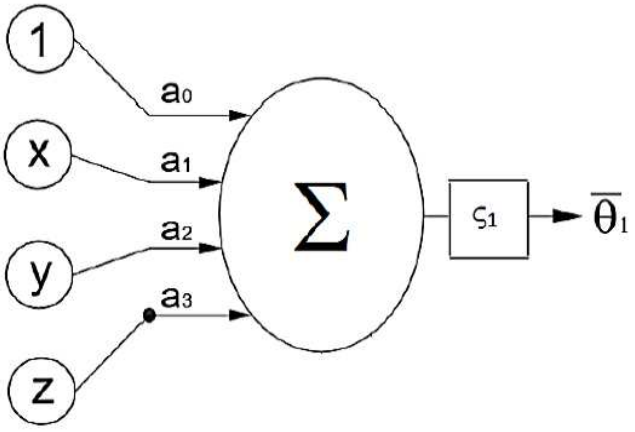

FIGURE 2. Structure of the nonlinear hypothesis.

where $i = 1, \ldots, m$, $j = 0, 1, 2, 3$, α is the modeling speed, $\varsigma_1^{i\prime}(\cdot)$, $\varsigma_2^{i\prime}(\cdot)$, $\varsigma_3^{i\prime}(\cdot)$, is the first derivative of the bounded map.

C. SECOND ORDER NONLINEAR HYPOTHESIS

The second order nonlinear hypothesis is described as the combination of the first order and second order terms and it is detailed as the sum of multiplications of the first order modeling parameters with the first and second order inputs.

A second order nonlinear hypothesis is described to relate the input variable of the end-effector $(x^i, y^i, z^i)^T$ with the output angles $(\theta_1^i, \theta_2^i, \theta_3^i)^T$ as:

$$\begin{aligned}\overline{\theta}_1^i &= \left\{a_0^i + a_1^i X_1^i + a_2^i X_2^i + a_3^i X_3^i\right.\\ &\quad \left. + a_4^i\left(X_1^i\right)^2 + a_5^i\left(X_2^i\right)^2 + a_6^i\left(X_3^i\right)^2\right\}\\ \overline{\theta}_2^i &= \left\{b_0^i + b_1^i X_1^i + b_2^i X_2^i + b_3^i X_3^i\right.\\ &\quad \left. + b_4^i\left(X_1^i\right)^2 + b_5^i\left(X_2^i\right)^2 + b_6^i\left(X_3^i\right)^2\right\}\\ \overline{\theta}_3^i &= \left\{c_0^i + c_1^i X_1^i + c_2^i X_2^i + c_3^i X_3^i\right.\\ &\quad \left. + c_4^i\left(X_1^i\right)^2 + c_5^i\left(X_2^i\right)^2 + c_6^i\left(X_3^i\right)^2\right\}\end{aligned} \tag{7}$$

where $i = 1, \ldots, m$, m is the data number, $X_0^i = 1$, $X_1^i = x^i$, $X_2^i = y^i$, $X_3^i = z^i$ are the inputs, $\overline{\theta}_1^i$, $\overline{\theta}_2^i$, $\overline{\theta}_3^i$ are estimated outputs, a_j^i, b_j^i, c_j^i, are modeling parameters to be updated, $j = 0, \ldots, 6$. The goal is to find the modeling parameters a_j^i, b_j^i, c_j^i, such that $\overline{\theta}_1^i$, $\overline{\theta}_2^i$, $\overline{\theta}_3^i$ are near to θ_1^i, θ_2^i, θ_3^i.

Figure 3 shows the structure of the second order nonlinear hypothesis for the output $\overline{\theta}_1^i$, it is similar for the outputs $\overline{\theta}_1^i$, $\overline{\theta}_3^i$.

The cost functions $J(a)$, $J(b)$, $J(c)$ are described as:

$$\begin{aligned}J(a) &= \frac{1}{2m}\sum_{i=1}^{m}\left(\overline{\theta}_1^i - \theta_1^i\right)^2\\ J(b) &= \frac{1}{2m}\sum_{i=1}^{m}\left(\overline{\theta}_2^i - \theta_2^i\right)^2\\ J(c) &= \frac{1}{2m}\sum_{i=1}^{m}\left(\overline{\theta}_3^i - \theta_3^i\right)^2\end{aligned} \tag{8}$$

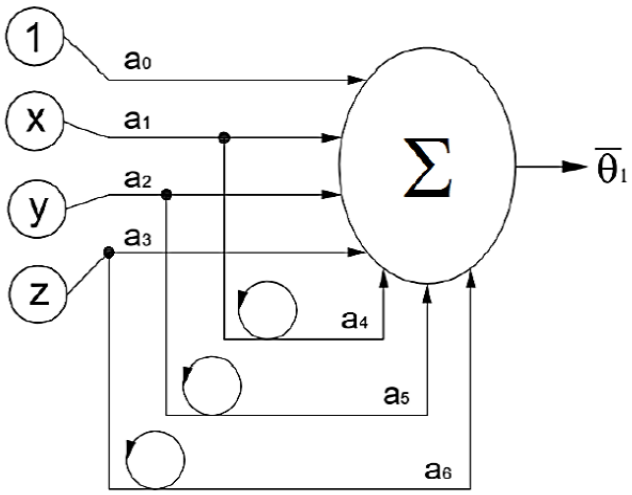

FIGURE 3. Structure of the second order nonlinear hypothesis.

Utilizing the gradient, the updating for a_j^i, b_j^i, c_j^i are as:

$$\begin{aligned} a_j^{i+1} &= a_j^i - \alpha \frac{\partial J(a)}{\partial a_j} = a_j^i - \frac{\alpha}{m} \sum_{i=1}^{m} \left(\overline{\theta}_1^i - \theta_1^i \right) X_j^i \\ b_j^{i+1} &= b_j^i - \alpha \frac{\partial J(b)}{\partial b_j} = b_j^i - \frac{\alpha}{m} \sum_{i=1}^{m} \left(\overline{\theta}_2^i - \theta_2^i \right) X_j^i \\ c_j^{i+1} &= c_j^i - \alpha \frac{\partial J(c)}{\partial c_j} = c_j^i - \frac{\alpha}{m} \sum_{i=1}^{m} \left(\overline{\theta}_3^i - \theta_3^i \right) X_j^i \end{aligned} \tag{9}$$

where $i = 1, \ldots, m$, $j = 0, 1, 2, 3$, α is the modeling speed, and:

$$\begin{aligned} a_j^{i+1} &= a_j^i - \alpha \frac{\partial J(a)}{\partial a_j} = a_j^i - \frac{\alpha}{m} \sum_{i=1}^{m} \left(\overline{\theta}_1^i - \theta_1^i \right) \left(X_j^i \right)^2 \\ b_j^{i+1} &= b_j^i - \alpha \frac{\partial J(b)}{\partial b_j} = b_j^i - \frac{\alpha}{m} \sum_{i=1}^{m} \left(\overline{\theta}_2^i - \theta_2^i \right) \left(X_j^i \right)^2 \\ c_j^{i+1} &= c_j^i - \alpha \frac{\partial J(c)}{\partial c_j} = c_j^i - \frac{\alpha}{m} \sum_{i=1}^{m} \left(\overline{\theta}_3^i - \theta_3^i \right) \left(X_j^i \right)^2 \end{aligned} \tag{10}$$

where $i = 1, \ldots, m$, $j = 4, 5, 6$.

D. NOVEL NONLINEAR HYPOTHESIS

The novel nonlinear hypothesis is described as the combination of the first order and second order terms and it is detailed as the sum of multiplications of the first order modeling parameters with the first and second order inputs, and multiplications of the first order modeling parameters with the cross first and second order inputs.

A novel nonlinear hypothesis is described to relate the input variable of the end-effector $(x^i, y^i, z^i)^T$ with the output angles $(\theta_1^i, \theta_2^i, \theta_3^i)^T$ as:

$$\begin{aligned} \overline{\theta}_1^i = \Big\{ & a_0^i + a_1^i X_1^i + a_2^i X_2^i + a_3^i X_3^i + a_4^i \left(X_1^i \right)^2 \\ & + a_5^i \left(X_2^i \right)^2 + a_6^i \left(X_3^i \right)^2 + a_7^i \left(X_1^i \right)^2 \left(X_2^i \right)^2 \\ & + a_8^i \left(X_2^i \right)^2 \left(X_3^i \right)^2 + a_9^i \left(X_2^i \right)^2 \left(X_3^i \right)^2 \\ & + a_{10}^i \left(X_1^i \right)^2 \left(X_2^i \right)^2 \left(X_3^i \right)^2 + a_{11}^i X_1^i X_2^i X_3^i \Big\} \\ \overline{\theta}_2^i = \Big\{ & b_0^i + b_1^i X_1^i + b_2^i X_2^i + b_3^i X_3^i + b_4^i \left(X_1^i \right)^2 \\ & + b_5^i \left(X_2^i \right)^2 + b_6^i \left(X_3^i \right)^2 + b_7^i \left(X_1^i \right)^2 \left(X_2^i \right)^2 \\ & + b_8^i \left(X_2^i \right)^2 \left(X_3^i \right)^2 + b_9^i \left(X_2^i \right)^2 \left(X_3^i \right)^2 \\ & + b_{10}^i \left(X_1^i \right)^2 \left(X_2^i \right)^2 \left(X_3^i \right)^2 + b_{11}^i X_1^i X_2^i X_3^i \Big\} \\ \overline{\theta}_3^i = \Big\{ & c_0^i + c_1^i X_1^i + c_2^i X_2^i + c_3^i X_3^i + c_4^i \left(X_1^i \right)^2 \\ & + c_5^i \left(X_2^i \right)^2 + c_6^i \left(X_3^i \right)^2 + c_7^i \left(X_1^i \right)^2 \left(X_2^i \right)^2 \\ & + c_8^i \left(X_2^i \right)^2 \left(X_3^i \right)^2 + c_9^i \left(X_2^i \right)^2 \left(X_3^i \right)^2 \\ & + c_{10}^i \left(X_1^i \right)^2 \left(X_2^i \right)^2 \left(X_3^i \right)^2 + c_{11}^i X_1^i X_2^i X_3^i \Big\} \end{aligned} \tag{11}$$

where $i = 1, \ldots, m$, m is the data number, $X_0^i = 1$, $X_1^i = x^i$, $X_2^i = y^i$, $X_3^i = z^i$ are the inputs, $\overline{\theta}_1^i$, $\overline{\theta}_2^i$, $\overline{\theta}_3^i$ are estimated outputs, a_j^i, b_j^i, c_j^i, are modeling parameters to be updated, $j = 0, \ldots, 11$. The goal is to find the modeling parameters a_j^i, b_j^i, c_j^i, such that $\overline{\theta}_1^i$, $\overline{\theta}_2^i$, $\overline{\theta}_3^i$ are near to θ_1^i, θ_2^i, θ_3^i.

Figure 4 shows the structure of the novel nonlinear hypothesis for the output $\overline{\theta}_1^i$, it is similar for the outputs $\overline{\theta}_1^i$, $\overline{\theta}_3^i$.

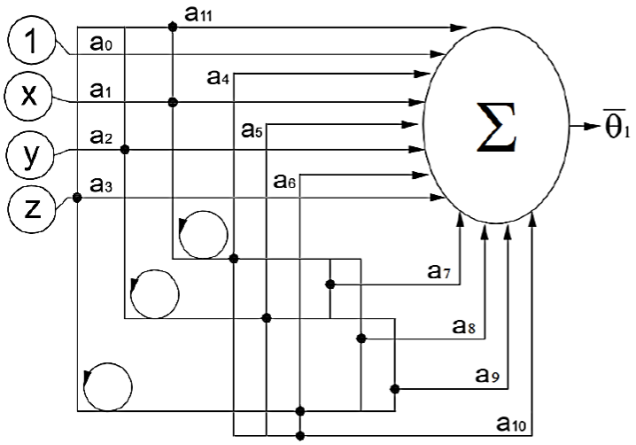

FIGURE 4. Structure of the novel nonlinear hypothesis.

The cost functions $J(a)$, $J(b)$, $J(c)$ are described as:

$$\begin{aligned} J(a) &= \frac{1}{2m} \sum_{i=1}^{m} \left(\overline{\theta}_1^i - \theta_1^i \right)^2 \\ J(b) &= \frac{1}{2m} \sum_{i=1}^{m} \left(\overline{\theta}_2^i - \theta_2^i \right)^2 \\ J(c) &= \frac{1}{2m} \sum_{i=1}^{m} \left(\overline{\theta}_3^i - \theta_3^i \right)^2 \end{aligned} \tag{12}$$

Utilizing the gradient, the updating for a_j^i, b_j^i, c_j^i are as:

$$\begin{aligned} a_j^{i+1} &= a_j^i - \alpha\frac{\partial J(a)}{\partial a_j} = a_j^i - \frac{\alpha}{m}\sum_{i=1}^{m}\left(\overline{\theta}_1^i - \theta_1^i\right)X_j^i \\ b_j^{i+1} &= b_j^i - \alpha\frac{\partial J(b)}{\partial b_j} = b_j^i - \frac{\alpha}{m}\sum_{i=1}^{m}\left(\overline{\theta}_2^i - \theta_2^i\right)X_j^i \\ c_j^{i+1} &= c_j^i - \alpha\frac{\partial J(c)}{\partial c_j} = c_j^i - \frac{\alpha}{m}\sum_{i=1}^{m}\left(\overline{\theta}_3^i - \theta_3^i\right)X_j^i \end{aligned} \quad (13)$$

where $i = 1, \ldots, m, j = 0, 1, 2, 3$, α is the modeling speed, and:

$$\begin{aligned} a_j^{i+1} &= a_j^i - \alpha\frac{\partial J(a)}{\partial a_j} = a_j^i - \frac{\alpha}{m}\sum_{i=1}^{m}\left(\overline{\theta}_1^i - \theta_1^i\right)\left(X_j^i\right)^2 \\ b_j^{i+1} &= b_j^i - \alpha\frac{\partial J(b)}{\partial b_j} = b_j^i - \frac{\alpha}{m}\sum_{i=1}^{m}\left(\overline{\theta}_2^i - \theta_2^i\right)\left(X_j^i\right)^2 \\ c_j^{i+1} &= c_j^i - \alpha\frac{\partial J(c)}{\partial c_j} = c_j^i - \frac{\alpha}{m}\sum_{i=1}^{m}\left(\overline{\theta}_3^i - \theta_3^i\right)\left(X_j^i\right)^2 \end{aligned} \quad (14)$$

where $i = 1, \ldots, m, j = 4, 5, 6$, and:

$$\begin{aligned} a_7^{i+1} &= a_7^i - \alpha\frac{\partial J(a)}{\partial a_7} = a_7^i - \frac{\alpha}{m}\sum_{i=1}^{m}\left(\overline{\theta}_1^i - \theta_1^i\right)\left(X_1^i\right)^2\left(X_2^i\right)^2 \\ b_7^{i+1} &= b_7^i - \alpha\frac{\partial J(b)}{\partial b_7} = b_7^i - \frac{\alpha}{m}\sum_{i=1}^{m}\left(\overline{\theta}_2^i - \theta_2^i\right)\left(X_1^i\right)^2\left(X_2^i\right)^2 \\ c_7^{i+1} &= c_7^i - \alpha\frac{\partial J(c)}{\partial c_7} = c_7^i - \frac{\alpha}{m}\sum_{i=1}^{m}\left(\overline{\theta}_3^i - \theta_3^i\right)\left(X_1^i\right)^2\left(X_2^i\right)^2 \end{aligned} \quad (15)$$

where $i = 1, \ldots, m, j = 7$, and:

$$\begin{aligned} a_8^{i+1} &= a_8^i - \alpha\frac{\partial J(a)}{\partial a_8} = a_8^i - \frac{\alpha}{m}\sum_{i=1}^{m}\left(\overline{\theta}_1^i - \theta_1^i\right)\left(X_1^i\right)^2\left(X_3^i\right)^2 \\ b_8^{i+1} &= b_8^i - \alpha\frac{\partial J(b)}{\partial b_8} = b_8^i - \frac{\alpha}{m}\sum_{i=1}^{m}\left(\overline{\theta}_2^i - \theta_2^i\right)\left(X_1^i\right)^2\left(X_3^i\right)^2 \\ c_8^{i+1} &= c_8^i - \alpha\frac{\partial J(c)}{\partial c_8} = c_8^i - \frac{\alpha}{m}\sum_{i=1}^{m}\left(\overline{\theta}_3^i - \theta_3^i\right)\left(X_1^i\right)^2\left(X_3^i\right)^2 \end{aligned} \quad (16)$$

where $i = 1, \ldots, m, j = 8$, and:

$$\begin{aligned} a_9^{i+1} &= a_9^i - \alpha\frac{\partial J(a)}{\partial a_9} = a_9^i - \frac{\alpha}{m}\sum_{i=1}^{m}\left(\overline{\theta}_1^i - \theta_1^i\right)\left(X_2^i\right)^2\left(X_3^i\right)^2 \\ b_9^{i+1} &= b_9^i - \alpha\frac{\partial J(b)}{\partial b_9} = b_9^i - \frac{\alpha}{m}\sum_{i=1}^{m}\left(\overline{\theta}_2^i - \theta_2^i\right)\left(X_2^i\right)^2\left(X_3^i\right)^2 \\ c_9^{i+1} &= c_9^i - \alpha\frac{\partial J(c)}{\partial c_9} = c_9^i - \frac{\alpha}{m}\sum_{i=1}^{m}\left(\overline{\theta}_3^i - \theta_3^i\right)\left(X_2^i\right)^2\left(X_3^i\right)^2 \end{aligned} \quad (17)$$

where $i = 1, \ldots, m, j = 9$, and:

$$\begin{aligned} a_{10}^{i+1} &= a_{10}^i - \alpha\frac{\partial J(a)}{\partial a_{10}} \\ &= a_{10}^i - \frac{\alpha}{m}\sum_{i=1}^{m}\left(\overline{\theta}_1^i - \theta_1^i\right)\left(X_1^i\right)^2\left(X_2^i\right)^2\left(X_3^i\right)^2 \\ b_{10}^{i+1} &= b_{10}^i - \alpha\frac{\partial J(b)}{\partial b_{10}} \\ &= b_{10}^i - \frac{\alpha}{m}\sum_{i=1}^{m}\left(\overline{\theta}_2^i - \theta_2^i\right)\left(X_1^i\right)^2\left(X_2^i\right)^2\left(X_3^i\right)^2 \\ c_{10}^{i+1} &= c_{10}^i - \alpha\frac{\partial J(c)}{\partial c_{10}} \\ &= c_{10}^i - \frac{\alpha}{m}\sum_{i=1}^{m}\left(\overline{\theta}_3^i - \theta_3^i\right)\left(X_1^i\right)^2\left(X_2^i\right)^2\left(X_3^i\right)^2 \end{aligned} \quad (18)$$

where $i = 1, \ldots, m, j = 10$, and:

$$\begin{aligned} a_{11}^{i+1} &= a_{11}^i - \alpha\frac{\partial J(a)}{\partial a_{11}} = a_{11}^i - \frac{\alpha}{m}\sum_{i=1}^{m}\left(\overline{\theta}_1^i - \theta_1^i\right)X_1^iX_2^iX_3^i \\ b_{11}^{i+1} &= b_{11}^i - \alpha\frac{\partial J(b)}{\partial b_{11}} = b_{11}^i - \frac{\alpha}{m}\sum_{i=1}^{m}\left(\overline{\theta}_2^i - \theta_2^i\right)X_1^iX_2^iX_3^i \\ c_{11}^{i+1} &= c_{11}^i - \alpha\frac{\partial J(c)}{\partial c_{11}} = c_{11}^i - \frac{\alpha}{m}\sum_{i=1}^{m}\left(\overline{\theta}_3^i - \theta_3^i\right)X_1^iX_2^iX_3^i \end{aligned} \quad (19)$$

where $i = 1, \ldots, m, j = 11$.

Remark 1: It is important to notice that in previous investigations, the nonlinear hypothesis of equations (4), (6) use the linear bounded maps. This document proposes two nonlinear hypothesis which use different structures instead of using the linear bounded maps. They are termed as novel nonlinear hypothesis of equations (11), (13), (14), (15), (16), (17), (18), (19) and second order nonlinear hypothesis of equations (11), (13), (14), (15), (16), (17), (18), (19) and their goal is to improve the second order processes modeling.

III. EXPERIMENTAL PLATFORM

A delta parallel robot has four degrees of freedom, three of them for the three-dimensional space translating movement of the effector and a fourth to control the orientation of the end effector, due to the configuration of the links that make up the mechanism, the platform of the end effector is always parallel to the base of the delta parallel robot. Figure 5 shows the main parts of our delta parallel robot of three degrees of freedom, it presents a Revolution-Revolution-Revolution (RRR) configuration, given that the variables of control correspond to the angles between the motor link and the fixed base of the mechanism.

Using our delta parallel robot shown in Figure 5, the experimental linear and curve paths are programmed, a control is implemented in an Arduino due development board and consists of 3 proportional integral controllers with pulse-width modulation (PWM) output (with a base frequency of 25×10^3 Hz to avoid unwanted vibration of the motors), which are tuned using the Zieglers-Nichols

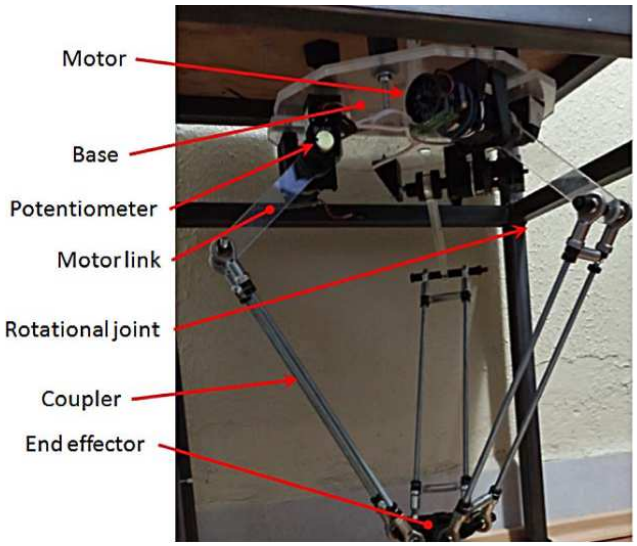

FIGURE 5. Main parts of our delta parallel robot.

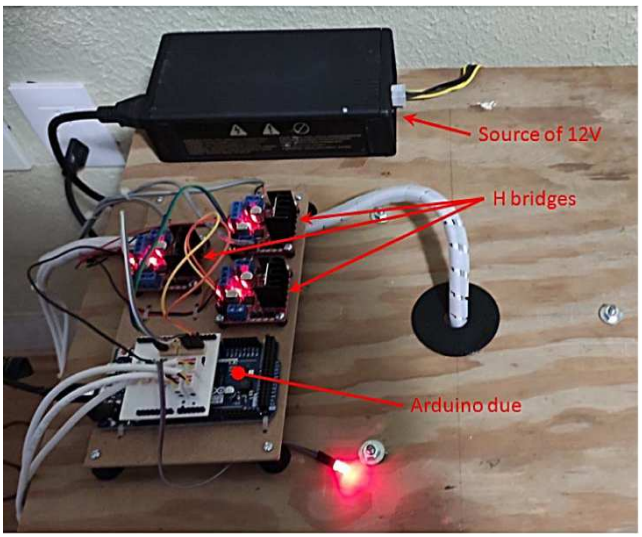

FIGURE 6. Electronic components of our delta parallel robot.

methodology in closed loop and 10×10^3 Ω linear potentiometers were used as feedback, on the other hand the motors (12 V) have a speed reducer with 60 : 1 ratio, while 4 H bridges L298N are used for the power interface; although each of these is capable of controlling up to two direct current motors, it is preferred to use one for each motor in order to avoid overheating the H bridges. Figure 6 shows the electronic components of our delta parallel robot.

An user program is developed in Python that allows to generate the experimental paths of the end effector of the delta parallel robot. Figure 7 shows the flow chart of the user program.

IV. EXPERIMENTAL RESULTS

In this section, the novel nonlinear hypothesis called NNH and second order nonlinear hypothesis called SONH of this document are compared with the nonlinear hypothesis of previous investigations [21], [22] called NH for modeling

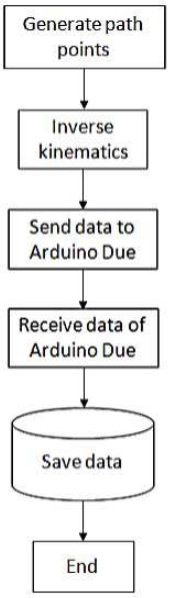

FIGURE 7. Flow chart of the user program.

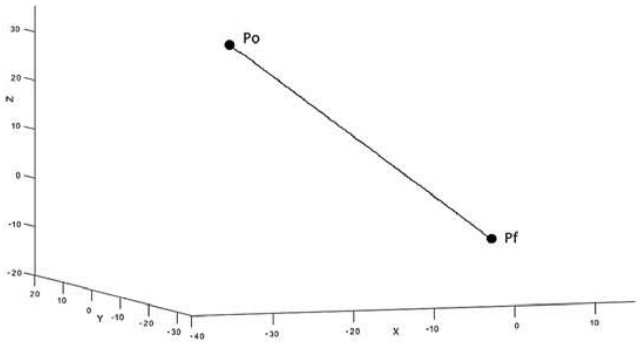

FIGURE 8. The experimental linear path.

of the experimental linear path called ELP and experimental curve path called ECP in a delta parallel robot. The goal is that the estimated outputs $\overline{\theta}_1^i$, $\overline{\theta}_2^i$, $\overline{\theta}_3^i$ should be near to the outputs $\theta_1^i, \theta_2^i, \theta_3^i$ and the cost functions $J(a), J(b), J(c)$ should be small. The ELP and ECP are selected for the comparison results; hence, other different paths could be used for the same goal with similar results.

A. LINEAR PATH

Selecting a starting point $P^o = (x^o; y^o; z^o) = (x^1; y^1; z^1)$ and a final point $P^f = (x^f; y^f; z^f) = (x^m; y^m; z^m)$, the parameterized equations of an ELP in three-dimensional space as a function of time t can be written as:

$$\begin{aligned} x^i &= x^1 + t\left(x^m - x^1\right) \\ y^i &= y^1 + t\left(y^m - y^1\right) \\ z^i &= z^1 + t\left(z^m - z^1\right) \end{aligned} \tag{20}$$

where x, y, z are in centimeters and t is in seconds. Figure 8 shows the ELP obtained with equation (20).

TABLE 1. Cost functions for the ELP.

Table I: Cost functions for the ELP			
Methods	**J(a)**	**J(b)**	**J(c)**
NH	0.3336	2.4074	0.1023
SONH	0.0537	0.0569	0.0266
NNH	0.0145	0.0281	0.0169

Before the training with equations (4), (6), and $\alpha = 1$, the initial parameters for the NH are in equation (21), rand is a random number with values between 0 and 1.

$$\begin{aligned} a &= [\text{rand, rand, rand, rand}]^T \\ b &= [\text{rand, rand, rand, rand}]^T \\ c &= [\text{rand, rand, rand, rand}]^T \end{aligned} \tag{21}$$

Before the training with equations (7), (9), (10), and $\alpha = 1$, the initial parameters for the SONH of this document are in equation (22), rand is a random number with values between 0 and 1.

$$\begin{aligned} a &= [\text{rand, rand, rand, rand, rand, rand, rand}]^T \\ b &= [\text{rand, rand, rand, rand, rand, rand, rand}]^T \\ c &= [\text{rand, rand, rand, rand, rand, rand, rand}]^T \end{aligned} \tag{22}$$

Before the training with equations (11), (13), (14), (15), (16), (17), (18), (19), and $\alpha = 1$, the initial parameters for the NNH of this document are in equation (23), rand is a random number with values between 0 and 1.

$$\begin{aligned} a &= [\text{rand, rand, rand, rand, rand, rand,} \\ &\quad \text{rand, rand, rand, rand, rand, rand}]^T \\ b &= [\text{rand, rand, rand, rand, rand, rand,} \\ &\quad \text{rand, rand, rand, rand, rand, rand}]^T \\ c &= [\text{rand, rand, rand, rand, rand, rand,} \\ &\quad \text{rand, rand, rand, rand, rand, rand}]^T \end{aligned} \tag{23}$$

Table 1 shows the cost functions $J(a)$ of (5), $J(b)$ of (8), $J(c)$ of (12) for the modeling of θ_1^i, θ_2^i, θ_3^i in an ELP during the training.

After the training with equations (4), (6), and $\alpha = 1$, the final parameters for the NH are in equation (24).

$$\begin{aligned} a &= [-5.2035, -35.9658, 36.7725, 37.0851]^T \\ b &= [-3.9967, -3.5788, 4.7108, 4.4442]^T \\ c &= [-14.2486, -28.4926, 30.2933, 29.9999]^T \end{aligned} \tag{24}$$

After the training with equations (7), (9), (10), and $\alpha = 1$, the final parameters for the SONH of this document are in equation (25).

$$\begin{aligned} a &= [-4.6120, 36.7327, 36.9275, -36.1591, \\ &\quad -2.4196, -2.1817, -2.4426]^T \\ b &= [-8.1301, 4.7920, 4.1345, -3.8051, \\ &\quad 16.2484, 16.6913, 16.5910]^T \\ c &= [-14.8846, 30.0773, 29.9877, -28.7174, \\ &\quad 2.7486, 2.8680, 2.0529]^T \end{aligned} \tag{25}$$

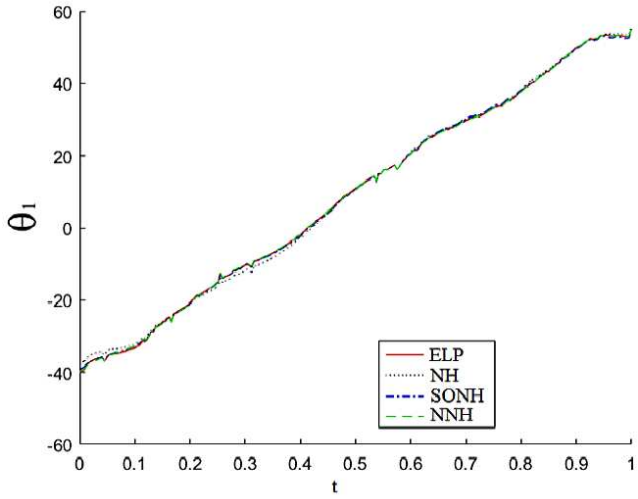

FIGURE 9. Modeling for θ_1 of an experimental linear path.

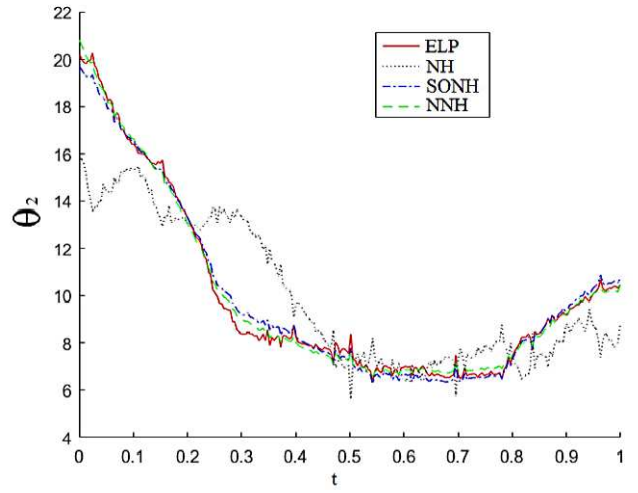

FIGURE 10. Modeling for θ_2 of an experimental linear path.

After the training with equations (11), (13), (14), (15), (16), (17), (18), (19), and $\alpha = 1$, the final parameters for the NNH of this document are in equation (26).

$$\begin{aligned} a &= [-4.5613, 36.5261, 35.939, -35.14, -3.0534, -2.7143, \\ &\quad -3.0323, 2.7521, 2.3571, 2.2612, 1.445, -14.7544]^T \\ b &= [-8.1311, 5.5969, 5.2089, -5.2069, 15.9037, 15.9643, \\ &\quad 15.6599, 4.6625, 4.3839, 3.8098, 1.7316, 21.8141]^T \\ c &= [-14.8432, 29.4209, 29.1562, 28.5380, 1.4909, 2.2351, \\ &\quad 1.9687, 3.2333, 2.8903, 3.3560, 1.6412, 11.0734]^T \end{aligned} \tag{26}$$

Figures 9, 10, 11 show the NH, SONH, and NNH for the modeling of θ_1^i, θ_2^i, θ_3^i in an ELP after the training where θ_1^i, θ_2^i, θ_3^i are in degree and t is in seconds.

From Figures 9, 10, 11, and Table 1, since $\overline{\theta}_1^i$, $\overline{\theta}_2^i$, $\overline{\theta}_3^i$ are the nearest to θ_1^i, θ_2^i, θ_3^i and the cost functions $J(a)$, $J(b)$, $J(c)$ are the smallest in the NNH, it can be observed the NNH reaches better performance than both the SONH and NH for

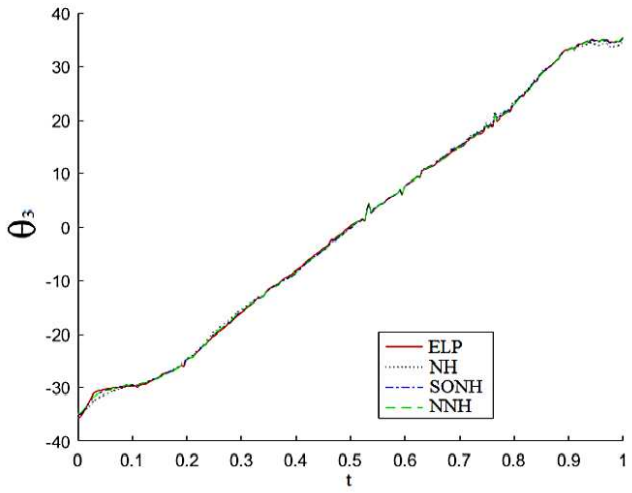

FIGURE 11. Modeling for θ_3 of an experimental linear path.

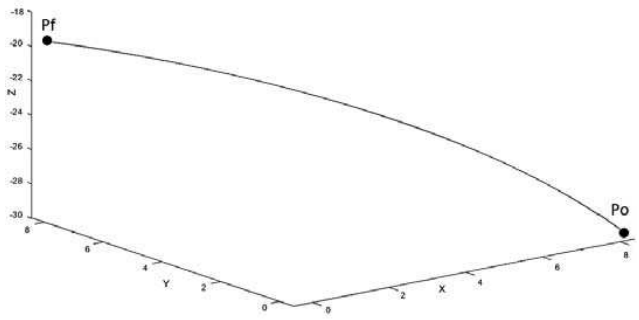

FIGURE 12. The experimental curve path.

the modeling of an ELP. Then the NNH is the best alternative for the modeling of an ELP.

B. CURVE PATH

Selecting a starting point $P^o = (x^o; y^o; z^o) = (x^1; y^1; z^1)$ and a final point $P^f = (x^f; y^f; z^f) = (x^m; y^m; z^m)$, the parameterized equations of an ECP in three-dimensional space as a function of time t can be written as:

$$\begin{aligned} x^i &= x^1 + rC\,(\omega t) \\ y^i &= y^1 + rS\,(\omega t) \\ z^i &= \left(z^1 - z^m\right) t \end{aligned} \tag{27}$$

where C is cosine, S is sine, r is the radius, ω is the angular velocity, x, y, z are in centimeters and t is in seconds. Figure 12 shows the ECP obtained with equation (27).

Before the training with equations (4), (6), and $\alpha = 1$, the initial parameters for the NH are in equation (21), rand is a random number with values between 0 and 1.

Before the training with equations (7), (9), (10), $\alpha = 1$, the initial parameters for the SONH of this document of are in equation (22), rand is a random number with values between 0 and 1.

Before the training with equations (11), (13), (14), (15), (16), (17), (18), (19), and $\alpha = 1$, the initial parameters for the NNH of this document are in equation (23), rand is a random number with values between 0 and 1.

TABLE 2. Cost functions for the ECP.

Methods	J(a)	J(b)	J(c)
NH	0.0136	0.0119	0.1874
SONH	0.0100	0.0160	0.0020
NNH	0.0065	0.0086	0.0019

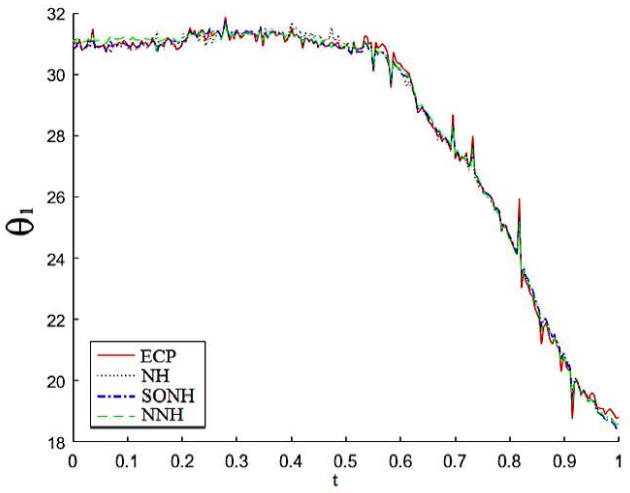

FIGURE 13. Modeling for θ_1 of an experimental curve path.

Table 2 shows the cost functions $J(a)$ of (5), $J(b)$ of (8), $J(c)$ of (12) for the modeling of θ_1^i, θ_2^i, θ_3^i in an ECP during the training.

After the training with equations (4), (6), and $\alpha = 1$, the final parameters for the NH are in equation (28).

$$\begin{aligned} a &= [15.7968, 19.1404, 2.0891, -13.2512]^T \\ b &= [-26.6402, 20.0150, -19.7215, -26.4806]^T \\ c &= [2.0498, 62.2792, 0.9871, -39.0685]^T \end{aligned} \tag{28}$$

After the training with equations (7), (9), (10), $\alpha = 1$, the final parameters for the SONH of this document are in equation (29).

$$\begin{aligned} a &= [16.6848, 13.6311, -4.5955, -10.1233, \\ &\quad -11.5888, 5.5343, -3.7544]^T \\ b &= [-24.4864, 19.8091, -21.6198, -21.6870, \\ &\quad -14.1592, 13.1037, -0.06419]^T \\ c &= [5.1496, 41.9544, -21.0604, -33.4090, \\ &\quad -29.0659, 5.7099, -10.5814]^T \end{aligned} \tag{29}$$

After the training with equations (11) , (13), (14), (15), (16), (17), (18), (19), and $\alpha = 1$, the final parameters for the NNH of this document are in equation (30).

$$\begin{aligned} a &= [16.6377, 13.8735, -4.2849, -9.6467, \\ &\quad -10.2981, 4.1885, -2.8381, -0.2291, \\ &\quad -2.3846, 0.8919, -0.1770, 4.9935]^T \\ b &= [-24.5127, 19.8641, -21.3004, -21.0702, \\ &\quad -12.1057, 11.0084, -0.2256, 0.2732, \\ &\quad -2.5322, 1.9621, -0.1237, 8.1622]^T \end{aligned}$$

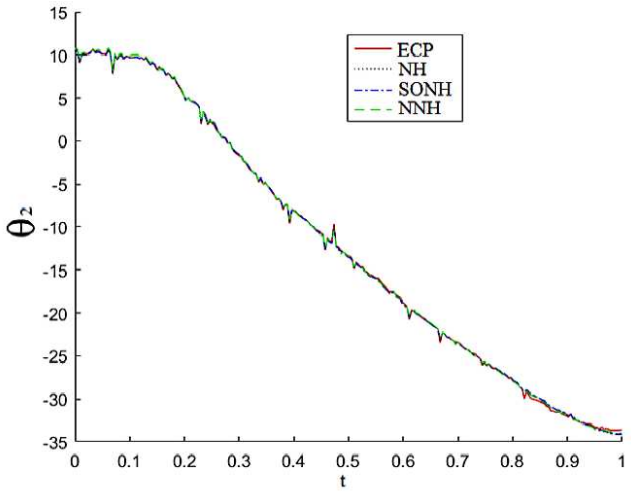

FIGURE 14. Modeling for θ_2 of an experimental curve path.

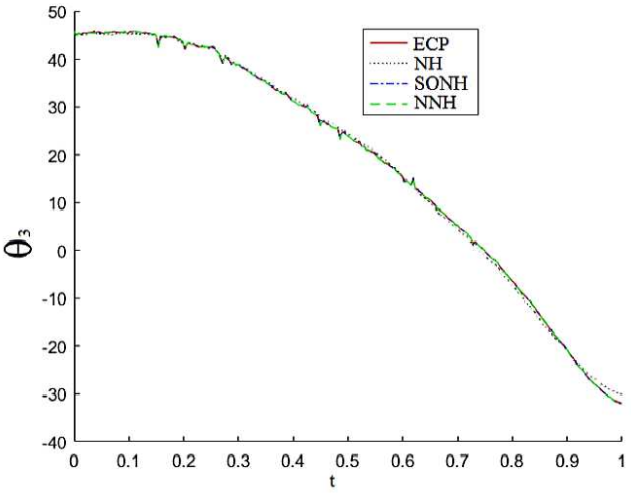

FIGURE 15. Modeling for θ_3 of an experimental curve path.

$$c = [5.1318, 41.6783, -21.2594, -32.3082, \\ -25.5617, 3.4821, -10.4259, -2.1242, \\ -6.4280, 0.1610, -0.6708, 10.8756]^T \quad (30)$$

Figures 13, 14, 15 show the NH, SONH, and NNH for the modeling of θ_1^i, θ_2^i, θ_3^i in an ECP after the training where θ_1^i, θ_2^i, θ_3^i are in degree and t is in seconds.

From Figures 13, 14, 15, and Table 2, since $\overline{\theta}_1^i$, $\overline{\theta}_2^i$, $\overline{\theta}_3^i$ are the nearest to θ_1^i, θ_2^i, θ_3^i and the cost functions $J(a)$, $J(b)$, $J(c)$ are the smallest in the NNH, it can be observed the NNH reaches better performance than both the SONH and NH for the modeling of an ECP. Then the NNH is the best alternative for the modeling of an ECP.

V. CONCLUSION

In this document, three kind of hypothesis were studied for the second order processes modeling: the nonlinear hypothesis of previous investigations, the second order nonlinear hypothesis, and the novel nonlinear hypothesis. The mentioned hypothesis were applied for the experimental linear and curve paths modeling in the delta parallel robot, since the estimated outputs were the nearest to the outputs and the cost functions were the smallest for the novel nonlinear hypothesis, the novel nonlinear hypothesis reached better performance than both the second order nonlinear hypothesis and nonlinear hypothesis of previous investigations. This method could be applied to other mechatronic processes as are medic, biologic, robotic, hydraulic, mechanic, and electronic. In the forthcoming work, other kind of nonlinear hypothesis will be designed, or the stability of the proposed method will be analyzed.

ACKNOWLEDGMENT

The authors would like to thank the editors and reviewers for important suggestions and comments to improve this research. They would also like to thank the Instituto Politécnico Nacional, the Consejo Nacional de Ciencia y Tecnología, the Secretaría de Investigación y Posgrado, and the Comisión de Operación y Fomento de Actividades Académicas for their support.

REFERENCES

[1] J. Wang, W.-C. Yeh, N. N. Xiong, J. Wang, X. He, and C.-L. Huang, "Building an improved Internet of Things smart sensor network based on a three-phase methodology," *IEEE Access*, vol. 7, pp. 141728–141737, 2019.
[2] J. Wang, N. N. Xiong, J. Wang, and W.-C. Yeh, "A compact ciphertext-policy attribute-based encryption scheme for the information-centric Internet of Things," *IEEE Access*, vol. 6, pp. 63513–63526, 2018.
[3] W. Zhu, W.-C. Yeh, N. N. Xiong, and B. Sun, "A new node-based concept for solving the minimal path problem in general networks," *IEEE Access*, vol. 7, pp. 173310–173319, 2019.
[4] C.-M. Lai, C.-C. Chiu, W.-C. Liu, and W.-C. Yeh, "A novel nondominated sorting simplified swarm optimization for multi-stage capacitated facility location problems with multiple quantitative and qualitative objectives," *Appl. Soft Comput.*, vol. 84, Nov. 2019, Art. no. 105684.
[5] W.-C. Yeh, "A new harmonic continuous simplified swarm optimization," *Appl. Soft Comput.*, vol. 85, Dec. 2019, Art. no. 105544.
[6] W.-C. Yeh, "Solving cold-standby reliability redundancy allocation problems using a new swarm intelligence algorithm," *Appl. Soft Comput.*, vol. 83, Oct. 2019, Art. no. 105582.
[7] Z. Du, Y. Kao, and J. H. Park, "New results for sampled-data control of interval type-2 fuzzy nonlinear systems," *J. Franklin Inst.*, vol. 357, no. 1, pp. 121–141, Jan. 2020.
[8] A. Mohammadi, S. H. Javadi, D. Ciuonzo, V. Persico, and A. Pescapé, "Distributed detection with fuzzy censoring sensors in the presence of noise uncertainty," *Neurocomputing*, vol. 351, pp. 196–204, Jul. 2019.
[9] J. M. Adánez, B. M. Al-Hadithi, and A. Jiménez, "Multidimensional membership functions in T-S fuzzy models for modelling and identification of nonlinear multivariable systems using genetic algorithms," *Appl. Soft Comput.*, vol. 75, pp. 607–615, Feb. 2019.
[10] J. Han, C. Yang, C.-C. Lim, X. Zhou, P. Shi, and W. Gui, "Power scheduling optimization under single-valued neutrosophic uncertainty," *Neurocomputing*, vol. 382, pp. 12–20, Mar. 2020.
[11] M. H. Haghighi, S. M. Mousavi, and V. Mohagheghi, "A new soft computing model based on linear assignment and linear programming technique for multidimensional analysis of preference with interval type-2 fuzzy sets," *Appl. Soft Comput.*, vol. 77, pp. 780–796, Apr. 2019.
[12] M. I. Jais, T. Sabapathy, M. Jusoh, R. B. Ahmad, M. H. Jamaluddin, M. R. Kamarudin, P. Ehkan, L. M. Loganathan, and P. J. Soh, "A fuzzy-based Angle-of-Arrival estimation system (AES) using radiation pattern reconfigurable (RPR) antenna and modified Gaussian membership function," *IEEE Access*, vol. 7, pp. 145477–145488, 2019.
[13] T.-L. Le, "Fuzzy C-Means clustering interval Type-2 cerebellar model articulation neural network for medical data classification," *IEEE Access*, vol. 7, pp. 20967–20973, 2019.
[14] L. Yang, Z. Liu, and Y. Chen, "Energy efficient walking control for biped robots using interval type-2 fuzzy logic systems and optimized iteration algorithm," *ISA Trans.*, vol. 87, pp. 143–153, Apr. 2019.

[15] K. Patan and M. Patan, "Neural-network-based iterative learning control of nonlinear systems," *ISA Trans.*, to be published, doi: 10.1016/j.isatra.2019.08.044.
[16] Y. Wang, Z. Pan, X. Yuan, C. Yang, and W. Gui, "A novel deep learning based fault diagnosis approach for chemical process with extended deep belief network," *ISA Trans.*, vol. 96, pp. 457–467, Jan. 2020.
[17] M. Kobayashi, "O(2)-valued hopfield neural networks," *IEEE Trans. Neural Netw. Learn. Syst.*, vol. 30, no. 12, pp. 3833–3838, Dec. 2019.
[18] P. Wan, D. Sun, M. Zhao, and S. Huang, "Multistability for almost-periodic solutions of takagi-sugeno fuzzy neural networks with nonmonotonic discontinuous activation functions and time-varying delays," *IEEE Trans. Fuzzy Syst.*, to be published, doi: 10.1109/TFUZZ.2019.2955886.
[19] Y. Shen, Z. Fang, Y. Gao, N. Xiong, C. Zhong, and X. Tang, "Coronary arteries segmentation based on 3D FCN with attention gate and level set function," *IEEE Access*, vol. 7, pp. 42826–42835, 2019.
[20] S. Xu, K. Liu, and X. Li, "A fuzzy process neural network model and its application in process signal classification," *Neurocomputing*, vol. 335, pp. 1–8, Mar. 2019.
[21] W. Ouyang, B. Xu, J. Hou, and X. Yuan, "Fabric defect detection using activation layer embedded convolutional neural network," *IEEE Access*, vol. 7, pp. 70130–70140, 2019.
[22] G. Zhang and Z. Zeng, "Stabilization of second-order memristive neural networks with mixed time delays via nonreduced order," *IEEE Trans. Neural Netw. Learn. Syst.*, vol. 31, no. 2, pp. 700–706, Feb. 2020.
[23] R. Krishnan, S. Jagannathan, and V. A. Samaranayake, "Direct error-driven learning for deep neural networks with applications to big data," *IEEE Trans. Neural Netw. Learn. Syst.*, to be published, doi: 10.1109/TNNLS.2019.2920964.
[24] Z. Qiumei, T. Dan, and W. Fenghua, "Improved convolutional neural network based on fast exponentially linear unit activation function," *IEEE Access*, vol. 7, pp. 151359–151367, 2019.
[25] F. Yu, L. Liu, L. Xiao, K. Li, and S. Cai, "A robust and fixed-time zeroing neural dynamics for computing time-variant nonlinear equation using a novel nonlinear activation function," *Neurocomputing*, vol. 350, pp. 108–116, Jul. 2019.
[26] Y. Zeng, L. Xiao, K. Li, J. Li, K. Li, and Z. Jian, "Design and analysis of three nonlinearly activated ZNN models for solving time-varying linear matrix inequalities in finite time," *Neurocomputing*, to be published, doi: 10.1016/j.neucom.2020.01.070.

GUSTAVO AQUINO received the Ph.D. degree from the Sección de Estudios de Posgrado e Investigación, ESIME Azcapotzalco, Instituto Politécnico Nacional, in 2020. He has published three articles in international journals. His fields of interest are robotic systems, modeling, and intelligent systems.

JOSÉ DE JESÚS RUBIO (Member, IEEE) is currently a full-time Professor with the Sección de Estudios de Posgrado e Investigación, ESIME Azcapotzalco, Instituto Politécnico Nacional. He has published over 134 international journal articles with 1964 cites from Scopus. He serves on the Editorial Board for the IEEE TRANSACTIONS ON NEURAL NETWORKS AND LEARNING SYSTEMS, the IEEE TRANSACTIONS ON FUZZY SYSTEMS, *Neural Computing and Applications*, the *Journal of Intelligent and Fuzzy Systems*, *Mathematical Problems in Engineering*, the *International Journal of Advanced Robotic Systems*, the IEEE LATIN AMERICA TRANSACTIONS, *Evolving Systems*, and the *International Journal of Business Intelligence and Data Mining*. He was a Guest Editor of *Computational Intelligence and Neuroscience*, from 2015 to 2016. He is also a Guest Editor of *Neurocomputing*, in 2019, *Applied Soft Computing*, in 2019, the *International Journal of Applied Mathematics and Computer Science*, in 2019, *Frontiers in Neurorobotics*, in 2019, the *Journal of Computational and Applied Mathematics*, in 2019, and *The Journal of Supercomputing*, in 2019. He has been the tutor of four P.Ph.D. students, 19 Ph.D. students, 42 M.S. students, four S. students, and 17 B.S. students.

JAIME PACHECO is currently a full-time Professor with the Sección de Estudios de Posgrado e Investigación, ESIME Azcapotzalco, Instituto Politécnico Nacional. He has published 25 articles in international journals. His fields of interest are robotic systems, modeling, and intelligent systems.

GUADALUPE JULIANA GUTIERREZ is currently a full-time Professor with the Sección de Estudios de Posgrado e Investigación, ESIME Azcapotzalco, Instituto Politécnico Nacional. She has published ten articles in international journals. Her fields of interest are robotic systems, modeling, and intelligent systems.

GENARO OCHOA received the Ph.D. degree from the Sección de Estudios de Posgrado e Investigación, ESIME Azcapotzalco, Instituto Politécnico Nacional, in 2017. He has published eight articles in international journals. His fields of interest are robotic systems, modeling, and intelligent systems.

RICARDO BALCAZAR received the Ph.D. degree from the Sección de Estudios de Posgrado e Investigación, ESIME Azcapotzalco, Instituto Politécnico Nacional, in 2017. He has published seven articles in international journals. His fields of interest are robotic systems, modeling, and intelligent systems.

DAVID RICARDO CRUZ received the Ph.D. degree from the Sección de Estudios de Posgrado e Investigación, ESIME Azcapotzalco, Instituto Politécnico Nacional, in 2018. He has published seven articles in international journals. His fields of interest are robotic systems, modeling, and intelligent systems.

ENRIQUE GARCIA received the Ph.D. degree from the Sección de Estudios de Posgrado e Investigación, ESIME Azcapotzalco, Instituto Politécnico Nacional, in 2017. He has published six articles in international journals. His fields of interest are robotic systems, modeling, and intelligent systems.

JUAN FRANCISCO NOVOA received the Ph.D. degree from the Sección de Estudios de Posgrado e Investigación, ESIME Azcapotzalco, Instituto Politécnico Nacional, in 2020. He has published seven articles in international journals. His fields of interest are robotic systems, modeling, and intelligent systems.

ALEJANDRO ZACARIAS is currently a full-time Professor with the Sección de Estudios de Posgrado e Investigación, ESIME Azcapotzalco, Instituto Politécnico Nacional. He has published ten articles in international journals. His fields of interest are robotic systems, modeling, and intelligent systems.